Corrosion inhibition of mild steel in NH_4Cl + NaOH environment containing *Azadirachta indica* leaf extract

P. Baitule and R. Manivannan*

Department of Chemical Engineering, National Institute of Technology Raipur, Chhattisgarh 492010, India
**E-mail: rmani.che@nitrr.ac.in*

Abstract

In this work, corrosion suppression of mild steel (MS) in the presence of 1 wt.% NH_4Cl + 1 wt.% NaOH solution using *Azadirachta indica* (neem) leaf extract was investigated. Weight loss studies of MS coupons immersed in different alkali concentrations, various immersion periods, and at various temperatures were carried out with and without inhibitor. The results showed that the effectiveness of the suppression increases with an increase in inhibitor concentration and was found to be a maximum of ~82% at 1000 ppm. Thermodynamic parameters were computed, including activation energy, enthalpy, and entropy (ΔS_a). A decrease in the activation energy (E_a) confirms that the corrosion inhibition (CI) process is physisorption and an enthalpy (ΔH_a) value of 66 kJ·mol^{-1} suggests that the inhibition process is endothermic. Among all the isotherms studied in this work, Langmuir adsorption isotherm was best fitted. Tafel plots showed that the corrosion current density (i_{corr}) value goes down with an increase in neem leaf extract (NLE) which corroborates a decline in corrosion rate (C_R) and an increase in inhibition efficiency (IE_{Tafel}). SEM pictures show that the protective coating on the metal has formed. Fe_2O_3, a stable oxide coating was established on the MS surface, lowering the C_R. Fourier transform infrared (FTIR) and X-ray photoelectron spectroscopy (XPS) analysis were conducted to understand the CI behaviour of NLE on MS. The phytochemical compounds in the NLE were detected, and the results of the metal coupon immersed in the extract were shifted, confirming an interaction between MS and extract that caused corrosion to be suppressed. According to XPS results, inhibitor molecules protect MS from oxidation, preventing over-oxidation of MS. NLE's anti-corrosion action is successfully supported by the finding that an inhibitor component creates a complex and thus hinders the corrosion of MS.

Received: July 23, 2023. Published: January 17, 2024 doi: 10.17675/2305-6894-2024-13-1-7

Keywords: *adsorption isotherm, Tafel plot, EIS, inhibition mechanism, FTIR, SEM.*

1. Introduction

Mild steel (MS) is employed for several applications in many industries. It is a highly significant engineering material for machinery as well as construction owing to its outstanding mechanical properties *viz*., malleability and ductility. MS is inexpensive and easily available [1]. For many engineering applications, MS is exposed to various aggressive environments *viz.,* acidic, alkaline, and salt solutions [2]. This causes corrosion and the

impact of corrosion makes the metal structure to get damaged. Hence, it is obligatory to avert the metal from corrosion with an eco-friendly technique [3]. There are different techniques to guard the metal from corrosion namely corrosion protection coating, anodic and cathodic protection, and green corrosion inhibitor (GCI) [4]. It has been shown that the film formed on metal behaves as a double-layer model in a basic medium. In an alkaline solution, strong passivation is formed on the metal surface. However, with the Cl^- solution, passivation is broken, resulting in increased C_R [5]. The most efficient way of reducing the deterioration of metal is by the addition of GCI. It is a good way to resolve the corrosion problem economically [6]. Because of their low cost, easy availability, economically viable, and high performance, inhibitors are more commonly used to minimize corrosion [7]. A corrosion inhibitor is an ingredient that shields the surface of a metal from a corrosive medium. While selecting the green corrosion inhibitor, the following factors should be considered such as corrosive medium composition, and metal characteristics [8]. *Azadirachta indica* is a classic tree, cultured in various regions of India [9]. Numerous studies have been implemented and researchers have kept continuous attention on neem plant usage for several pharmacologic applications due to its medicinal properties [10]. This plant extract holds high volumes of a water-soluble, electrochemically active compound. Neem leaves have an unpleasant (bitter) taste because of triterpenes or limonoids [11]. Neem leaf inhibitor was used as GCI to retard MS corrosion in an acidic environment (HCl, H_2SO_4, and HNO_3) because of its antioxidant properties. While there is a lot of literature on acidic media, there are very few publications on the alkaline medium [12]. Corrosion issues due to ammonium chloride (NH_4Cl) are a problem in oil refineries. The corrosion caused by NH_4Cl is mostly observed in crude unit overhead streams, fractionator streams, and reactor effluent in hydro-processing units. Corrosion causes leakage of combustible gases and oils, particularly in high-pressure reactor effluent streams, which can result in major failures including fire and explosion [13]. The potential of mature areca nut husk (MAH) extract to suppress corrosion on Cu and MS in acid and alkaline mediums was investigated. The corrosive medium tested in this study included sodium hydroxide and hydrochloric acid solution. The maximum inhibition efficiency (*IE*) was reported as ~94% and ~91% for MS, and copper, and ~93% and ~90% in acidic and alkaline medium respectively [14]. Henna and zeolite powder were tested for the CI property of MS in sodium hydroxide solution. With an increase in plant extract concentration, inhibition effectiveness increased. The *IE* was observed to be ~95% at 30°C [15]. Sweet prayer (*Thaumatococcus danielli*) leaf extract was used as a GCI to protect against MS corrosion in NaOH solution. The *IE* was found to be inversely related to temperature from 298 K to 333 K. Maximum *IE* of 90% was attained with 1 g/L of the extract [16].

In this work, sodium hydroxide was used as a corrosive medium with ammonium chloride as the chloride ion source. Predetermined concentrations, from the screening experiments, were used in this work. The current work investigates the inhibitive properties of neem leaf extract as a GCI for MS in an alkaline medium (1 wt.% NH_4Cl + 1 wt.% NaOH). Weight loss studies, Tafel measurements, and EIS were employed to determine the

inhibitory efficacy of the neem leaf inhibitor. SEM was used to inspect the surface morphology of the MS coupon dipped in the alkaline medium without and with neem leaf extract. FTIR (Fourier transform infrared) analysis was performed for neem leaf powder to recognize the phytochemical compounds in neem leaf extract, which is essential to minimize metal corrosion.

2. Experimental Procedure

2.1. Sample preparation

The composition of the MS coupon used in this study was determined using optical emission spectrometry (SPECTROMAXx, Ametek Germany) and the results are presented in Table 1. In this study, an MS coupon with dimensions of 2.25 cm diameter and 1 cm thickness was employed. Before each run, the sample was polished with sandpaper of various grades, washed and cleaned with acetone and distilled water (DW) and subsequently dried with hot air. The suppressive effect of plant extract was studied by immersion of coupon into 1 wt.% NH_4Cl + 1 wt.% NaOH solution. The corrosion inhibitory effect on MS at various temperatures was studied without and with an inhibitor (1000 ppm) for 10 min. Coupons were kept in a desiccator when not in use.

Table 1. Composition of MS coupon used in this study.

Elements	C	Si	Mn	P	S	Cr	Cu	Fe
Composition (wt.%)	0.253	0.051	0.455	0.018	0.0160	0.022	0.045	Balance

2.2. Preparation of NLE

Neem leaves were washed with water to take away the contaminants followed by drying them in shade. Subsequently, neem leaves were dried and then processed in a mixer-grinder to make a very fine powder. 100 g of *Azadirachta indica* leaf powder was mixed with 500 mL of CH_3OH and kept for a day. The resulting blend was refluxed at 50–60°C for 5 h. The refluxed solution was concentrated in a vacuum evaporation setup. The resulting thick liquor (extract) was then used for the preparation of various concentrations of the inhibitor to analyze its corrosion-inhibitive properties.

2.3. Weight loss studies

Experiments were executed by immersing the MS coupons in various concentrations, immersion times, and temperatures of alkali solution with and without NLE. Subsequently, the MS coupons were withdrawn from the alkaline medium, washed with acetone and DW and then dried with hot air. The samples were weighed pre- and post-submersion in the test solution (1 wt.% NH_4Cl + 1 wt.% NaOH) with and without NLE. The duration of immersion

was 10 min. Measurable weight loss was obtained for 10 min. All tests were conducted thrice with the average C_R values calculated using the standard formula reported elsewhere [17]. The inhibition efficiency (*IE*) was evaluated using the below formula.

$$IE(\%) = \frac{w_a - w_p}{w_a} \cdot 100 \quad (1)$$

where, w_p and w_a are the weight loss of the samples taken from the medium with and without NLE respectively.

Corrosion rate (C_R) in mm/y was calculated using the below Eq. 2 [17]

$$C_R = \frac{87.6w}{\rho At} \quad (2)$$

where, w = weight loss of coupon (mg), ρ = mild steel density (g cm^{-3}), t = immersion time (h), and A = area of coupon (cm^2) immersed in 1 wt.% NH_4Cl + 1 wt.% NaOH solution. Surface coverage (θ) was obtained by the following formula (Eq. 3) [18, 19]

$$\theta = \frac{IE}{100} \quad (3)$$

The above equation is only applicable to inhibitors with blocking action [20].

2.4. Electrochemical experiments

Potentiostat (Parstat, USA) instrument was used for conducting the electrochemical runs and the cell contained three electrodes: a saturated Ag/AgCl electrode (reference), a platinum (Pt) wire (counter), and MS electrode (working). Each electrochemical run was performed in 1 wt.% NH_4Cl + 1 wt.% NaOH solution without and with plant extract of several concentrations. Before the start of experiments, the MS electrode was polished with sandpaper, washed with DW and again polished with various grades of Al_2O_3. For Tafel investigations, a potential span of –250 mV to +250 mV over open circuit potential (OCP) was applied at a scan speed of 1 mV/s. i_{corr} and E_{corr} values were computed by extrapolating Tafel graphs. EIS studies were carried out at OCP with 10 mV amplitude and frequency between 10^5 Hz and 0.1 Hz.

2.5. Characterization techniques

MS specimens were submerged in 1 wt.% NH_4Cl + 1 wt.% NaOH solution with (1000 ppm) and without inhibitor (0 ppm) for 6 h and then it was dried and utilized for surface analysis *viz*., SEM and XPS analysis. FTIR analysis of ground neem leaf powder was performed to ascertain the functional groups that existed in the powder.

3. Results and Discussion

3.1. Gravimetric studies

3.1.1. Effect of NaOH concentration on C_R

Gravimetric studies were conducted to assess MS corrosion in an alkaline medium. The C_R of MS immersed in a 1 wt.% NH_4Cl with varying NaOH concentrations is presented in Figure 1. The result disclosed that the C_R increases with an increase in NaOH concentrations. This could be due to the intensification in the aggressiveness of the corrosion ions in attacking the surface. pH of the solutions ranged between 12.2 (with inhibitor) and 12.5 (without inhibitor).

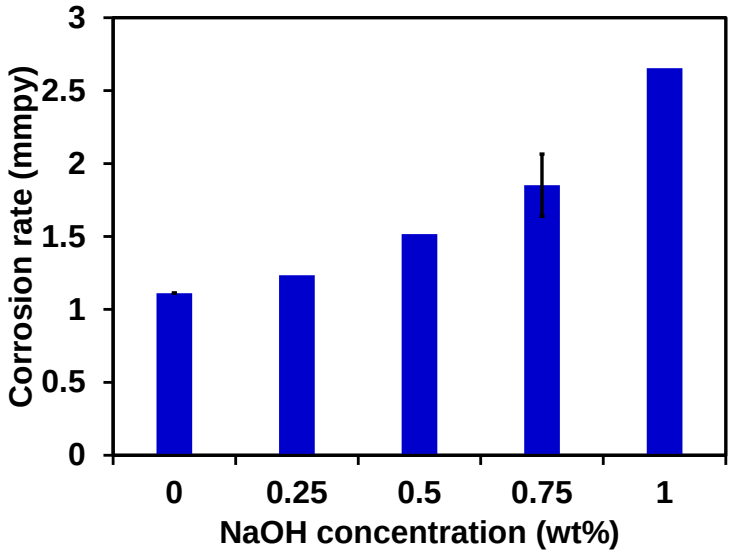

Figure 1. Effect of NaOH concentration on MS corrosion rate with 1 wt.% NH_4Cl solution.

3.1.2. Effect of NLE concentration on IE

Figure 2 illustrates the corrosion *IE* of MS in wt.% NH_4Cl + 1 wt.% NaOH solution with various inhibitor concentrations. *IE* ascends along with an increase in plant extract concentration. A higher *IE* of 82% was obtained with 1000 ppm plant extract. Inhibitor concentration beyond 1000 ppm did not show a significant increase in efficiency. Hence, the inhibitor concentration of 1000 ppm was selected for further study.

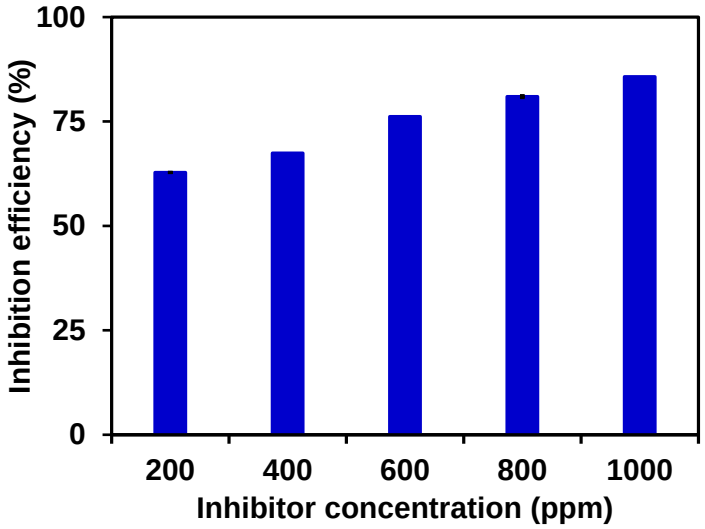

Figure 2. Effect of *Azadirachta indica* leaf extract concentration on MS corrosion *IE* with 1 wt.% NH_4Cl + 1 wt.% NaOH solution.

3.1.3. Effects of immersion time on IE and C_R

Figure 3(a) depicts the influence of submersion time on C_R of MS in 1 wt.% NH_4Cl + 1 wt.% NaOH medium without and without 1000 ppm of NLE. Results disclosed that the C_R of MS increases with an increase in submersion time. The C_R of MS was seen to be marginal with NLE. Figure 3(b) shows that *IE* decreases with an increase in the submersion period. This could be due to the dissolution of the adsorbed species for longer immersion times [21].

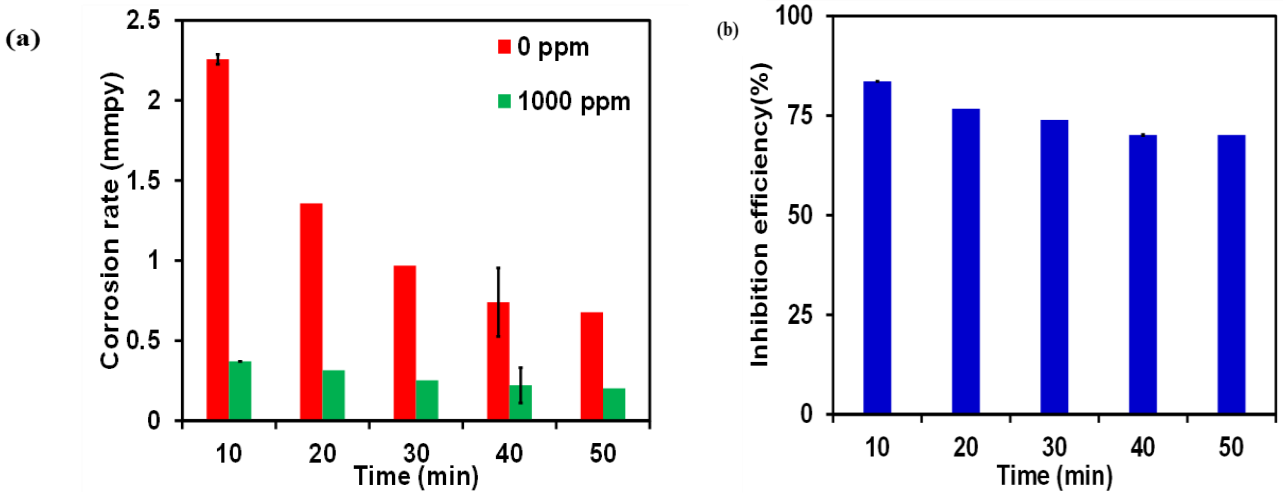

Figure 3. Effect of submersion time on **(a)** C_R of MS in 1 wt.% NH_4Cl + 1 wt.% NaOH without and with 1000 ppm *Azadirachta indica* leaf extract concentration and **(b)** inhibition efficiency.

3.1.4. Effect of temperature on C_R and IE

The influence of temperature on the C_R of MS in 1 wt.% NH_4Cl + 1 wt.% NaOH solution was examined with and without 1000 ppm of extract and the obtained results are presented

in Figure 4. As shown in Figure 4(a), C_R drops as the temperature of the medium with inhibitor ascends from 30°C to 60°C. The *IE* drops with temperature, as seen in Figure 4(b). The higher dissolution of metal at high temperatures, and the desorption of adhered *Azadirachta indica* leaf extract molecules from MS surfaces, are responsible for the decline in *IE*. Higher temperatures promote the dissolution of MS and cause the inhibitor molecules that have been attached to the metal to desorb.

The Arrhenius relation (Eq. 4) can be used to evaluate the activation energy (E_a)

$$\log(C_R) = -\frac{E_a}{2.303RT} + A' \tag{4}$$

where R, T and A' denote universal gas constant, abs. temperature (K), and Arrhenius constant respectively.

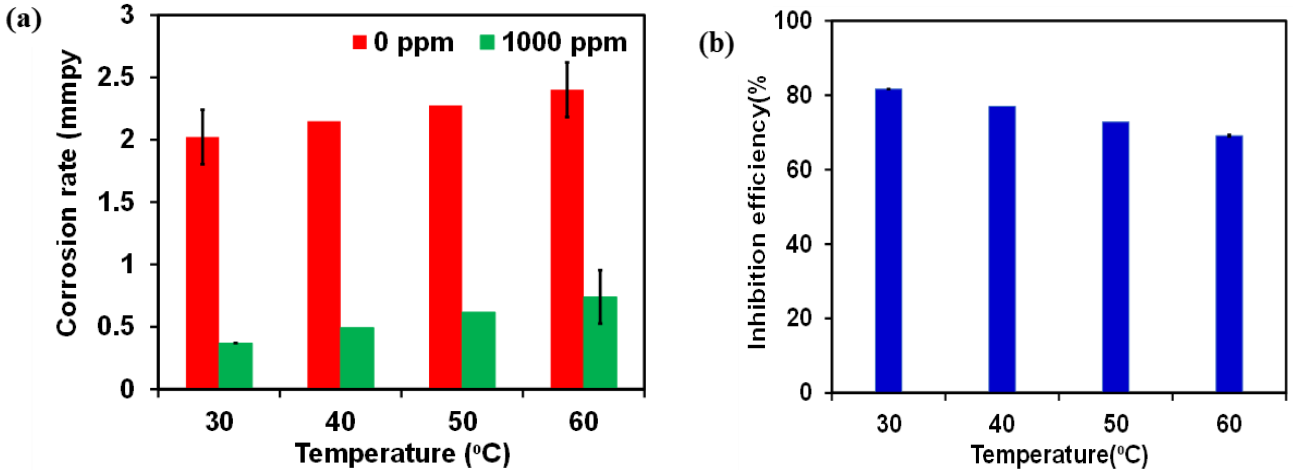

Figure 4. Effect of temperature on MS **(a)** C_R in 1 wt.% NH_4Cl + 1 wt.% NaOH without (0 ppm) and with 1000 ppm *Azadirachta indica* leaf extract **(b)** corrosion *IE*.

Arrhenius plot of MS in 1 wt.% NH_4Cl + 1 wt.% NaOH solution with and without inhibitor is shown in Figure 5. With inhibitor, the *Azadirachta indica* leaf extract molecules get adhered strongly onto the MS surface. However, the literature suggests that $E_a < 40$ kJ/mol indicates physisorption, and those with a value >80 kJ/mol specify chemisorption. E_a values were 5 kJ/mol and 19 kJ/mol at 0 ppm and 1000 ppm respectively. As both the values are below 40 kJ/mol, the *Azadirachta indica* leaf extract follows a physical adsorption mechanism. Compared to the uninhibited solution, supplementation of *Azadirachta indica* leaf extract caused E_a to increase. Change in enthalpy (ΔH_a) and entropy (ΔS_a) was evaluated using transition state Eq. 5:

$$\log\frac{C_R}{T} = \log\frac{R}{Nh} + \frac{\Delta S_a}{2.303R} - \frac{\Delta H_a}{2.303RT} \tag{5}$$

where, h denotes Planck's constant, and N specifies Avogadro's number.

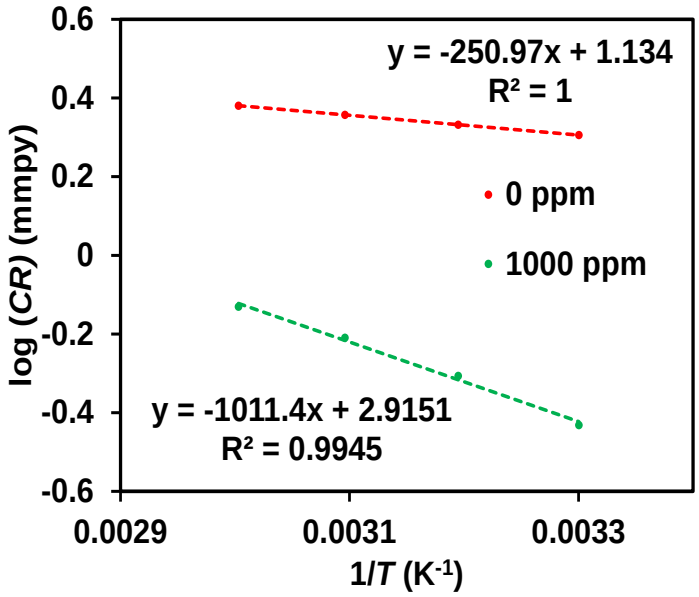

Figure 5. Arrhenius plot of MS in 1 wt.% NH_4Cl + 1 wt.% NaOH without (0 ppm) and with (1000 ppm) *Azadirachta indica* leaf extract.

Figure 6 displays $\log(C_R/T)$ against $1/T$ plot in the form of straight lines with a slope of $-\frac{\Delta H_a}{2.303RT}$ and $\log\frac{R}{Nh}+\frac{\Delta S_a}{2.303R}$ as the intercept. The endothermic nature of the metal dissolution process is reflected by the positive values of ΔH_a (9 kJ/mol at 0 ppm and 66 kJ/mol at 1000 ppm). The increase in *Azadirachta indica* extract-related ΔH_a indicates kinetics of activation, which plays a major role in controlling the reduction in MS C_R [22].

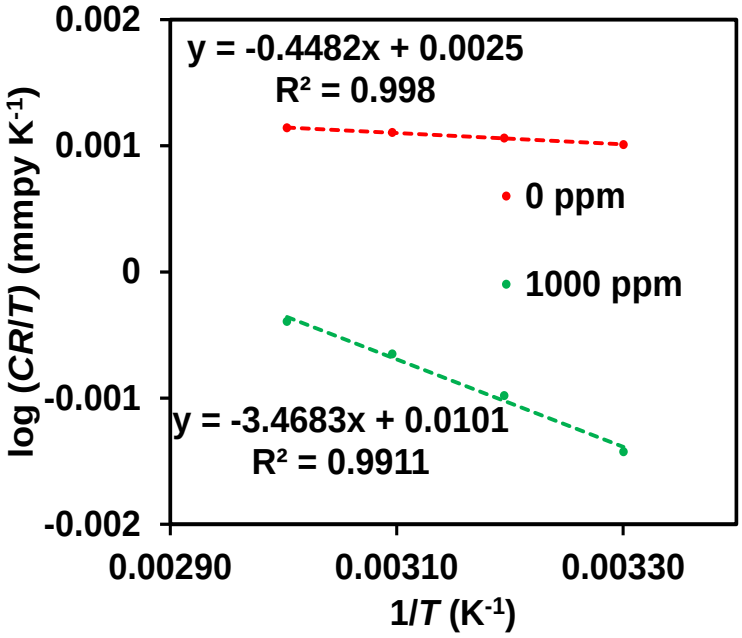

Figure 6. The plot of log (C_R/T) *vs.* $1/T$ of MS in 1 wt.% NH_4Cl + 1 wt.% NaOH with and without 1000 ppm *Azadirachta indica* leaf extract.

The high negative activation entropy values reveal that disorderliness reduces with the progression of reactant molecules to complexes. Also, this corroborates that the rate depends on associations instead of a dissociation step. The increase of ΔS_a (–176 J/mol·K and –142 J/mol·K at 0 ppm and 1000 ppm respectively) with the increase in inhibitor concentration indicates that disorderliness increases as one proceeds from reactant to complex formed. This behaviour could be interpreted with the displacement of molecules of water during *Azadirachta indica* extract adsorption on MS surfaces [23].

At constant pressure, Q_{ads} equals the enthalpy of adsorption (ΔH_{ads}). Eq. 6 was used to compute Q_{ads} at a constant *Azadirachta indica* extract concentration.

$$\log\frac{\theta}{1-\theta} = \log A'' + \log C - \frac{Q_{ads}}{2.303RT} \tag{6}$$

where C signifies the concentration of *Azadirachta indica* leaf extract (ppm), θ signifies surface coverage, and A'' signifies a constant. A plot between $\log\frac{\theta}{1-\theta}$ and $1/T$ constructed with 1000 ppm inhibitor concentration is shown in Figure 7. Straight line slope is given by $-\Delta H_{ads}/2.303R$. ΔH_{ads} was determined as –19 kJ·mol^{-1}. A negative ΔH_{ads} indicates that the plant extract adsorbed on metal is an exothermic reaction and a negative value ΔH_{ads} might be either physical adsorption or chemical adsorption. ΔH_{ads} values ≤42 kJ·mol^{-1} indicate physical adsorption, whereas 100 kJ·mol^{-1} or higher signifies chemisorption [24].

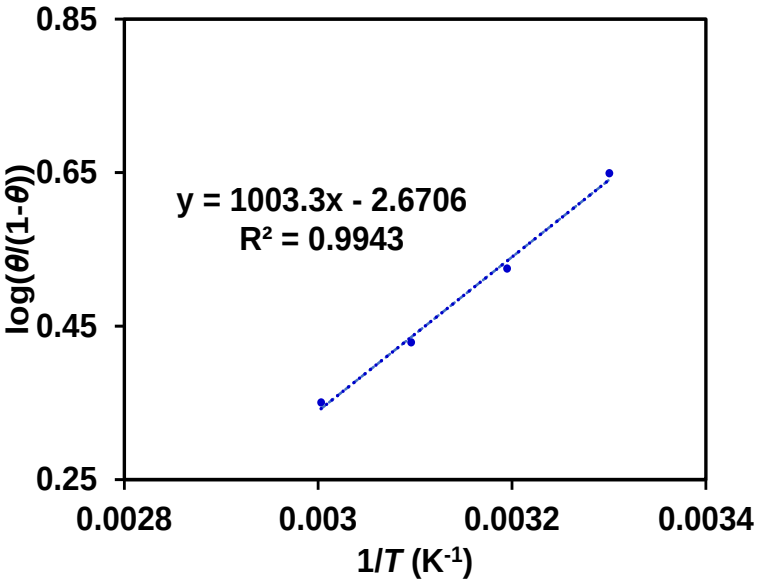

Figure 7. The plot of $\log(\theta/1-\theta)$ *vs.* $1/T$ of MS in 1 wt.% NH_4Cl + 1 wt.% NaOH with 1000 ppm *Azadirachta indica* leaf extract.

3.2. Potentiodynamic polarization studies (Tafel studies)

Figure 8 depicts potentiodynamic polarization plots of MS subjected to varying inhibitor concentrations. Tafel constant such as E_{corr}, and i_{corr}, was found from potentiodynamic plots

and results are summarized in Table 2. The inhibition efficiency of Tafel (IE_{Tafel}) studies was calculated from i_{corr} values using (Eq. 7).

$$IE_{\text{Tafel}}(\%) = \frac{i^{\text{a}}_{\text{corr}} - i^{\text{p}}_{\text{corr}}}{i^{\text{a}}_{\text{corr}}} \quad (7)$$

$i^{\text{a}}_{\text{corr}}$ denotes the i_{corr} without inhibitor whereas $i^{\text{p}}_{\text{corr}}$ denotes the i_{corr} with inhibitor at a specific concentration.

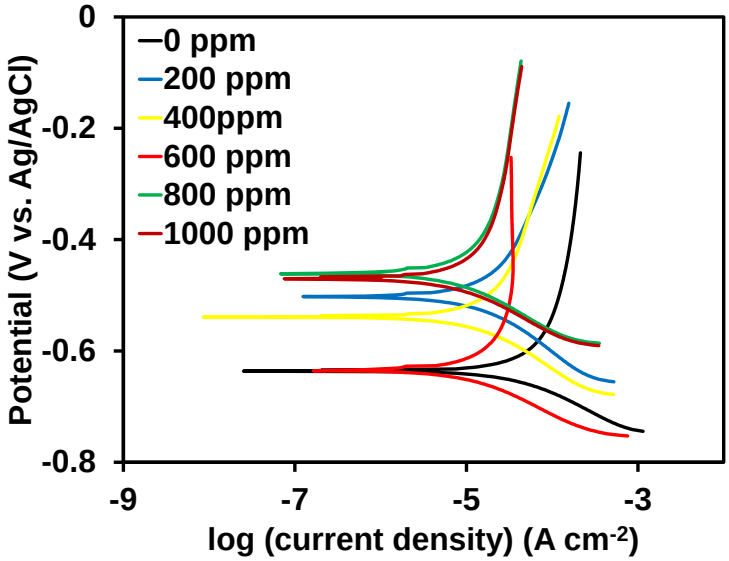

Figure 8. Tafel plots of MS in 1 wt.% NH_4Cl + 1 wt.% NaOH with various concentrations of *Azadirachta indica* leaf extract.

Table 2 reveals that the i_{corr} descends with ascends in inhibitor concentration, which indirectly denotes a decrease in C_R. The corrosion potential (E_{corr}) becomes more negative with ascends in plant extract concentration which corresponds to the characteristics of a mixed inhibitor [25]. The IE_{Tafel} ascends with an ascend in inhibitor concentration. From Tafel plots, it is clear that i_{corr} is inversely proportional to inhibitor concentration [26]. It is quite obvious that IE_{Tafel} increases as plant extract concentration increases. The highest IE_{Tafel} of ~85% was found at a concentration of 1000 ppm. A similar pattern was reported in the CI of MS in 0.5 M NaOH medium [14]. *Aquilaria crassna* leaves with 1 M HCl also resulted in the same pattern [27].

Table 2. Potentiodynamic parameters and IE_{Tafel} of MS in 1 wt.% NH_4Cl + 1 wt.% NaOH solution with different concentrations of inhibitor.

Sr. No.	Concentration (ppm)	E_{corr} (mV *vs.* Ag/AgCl)	i_{corr} (μA/cm²)	C_R (mmpy)	IE_{Tafel} (%)
1	0	–629.7	46.9	0.54	0
2	200	–492.7	11.5	0.13	76

Sr. No.	Concentration (ppm)	E_{corr} (mV *vs.* Ag/AgCl)	i_{corr} (μA/cm²)	C_R (mmpy)	IE_{Tafel} (%)
3	400	–532.3	10.9	0.12	78
4	600	–632.5	9.8	0.11	80
5	800	–440.8	8.1	0.09	83
6	1000	–462.8	7.0	0.08	85

3.3. Electrochemical impedance spectroscopy experiments

Kramers–Kronig transformation (KKT) is the mathematical relationship between imaginary and real parts of impedance that must be followed by impedance data and may be checked for causality, linearity, and stability. KKT can be represented by the following equations (Eq. 8 and 9)

$$Z'(\omega) = \frac{2\omega}{\pi}\int_0^\infty \frac{z'(x) - z'(\omega)}{x^2 - \omega^2}\mathrm{d}x \tag{8}$$

$$Z'(\omega) = Z'(\infty) + \frac{2}{\pi}\int_0^\infty \frac{xz'(x) - \omega z''(\omega)}{x^2 - \omega^2}\mathrm{d}x \tag{9}$$

where Z' be the real impedance values and Z'' be the imaginary impedance values and ω be can be calculated using the following correlation, $\omega = 2\pi f$, where $Z(\omega)$ represents the impedance and f stands for frequency in Hertz,

In Eqs. 8 and 9, the integral value is computed with the $Z(\omega)$ based on experimental data obtained over a certain frequency range (ω_{min}, ω_{max}) [28].

Figures 9A and 9B depict the KKT validation plots for the Z_{re} and Z_{im} values. The plots show a good match between the experimental and calculated data.

Figure 10 displays the Nyquist plots of MS in 1 wt.% NH_4Cl + 1 wt.% NaOH at various inhibitor concentrations. EIS experimental data were modelled with an electrical equivalent circuit (EEC) using ZsimpWin software and the fitted circuit is presented in Figure 11.

EEC consists of 3 resistances and 2 CPE (constant phase elements) *i.e.*, (R(Q(R(QR))) as indicated in Figure 11. In the EEC, R_{ct} denotes charge transfer resistance and R_{sol} denotes solution resistance. R_f and CPE_f represent the film resistance and film capacitance adhered to the metal surface and CPE_{dl} represents double-layer capacitance at the metal–solution interface.

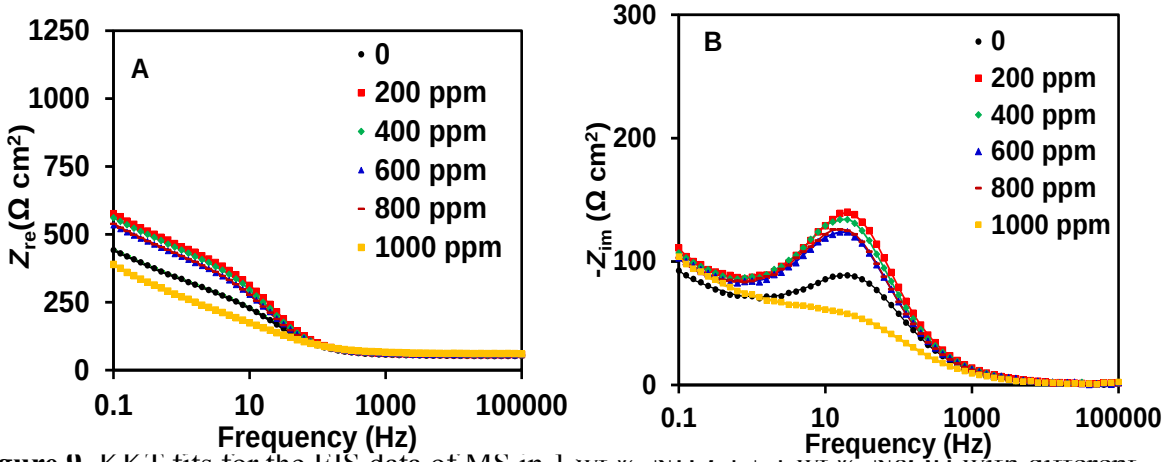

Figure 9. KKT fits for the EIS data of MS in 1 wt.% NH_4Cl + 1 wt.% NaOH with different concentrations of *Azadirachta indica* leaf extract. Solid lines denote the KKT fit and the marker denotes the experimental data. (A) Z_{re} *vs*. frequency (B) $-Z_{im}$ *vs*. frequency.

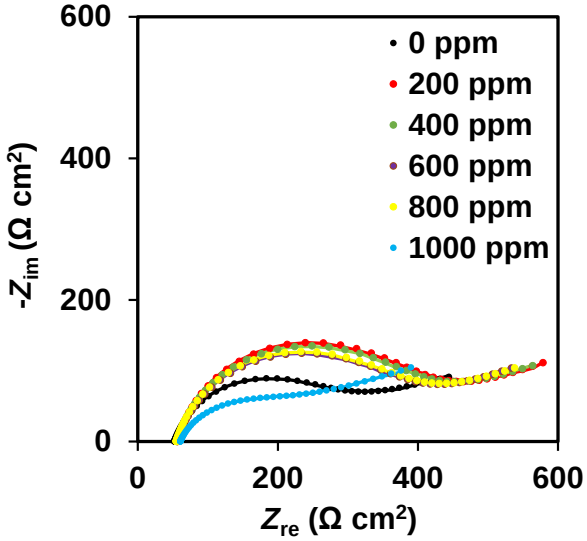

Figure 10. Nyquist plots of MS in 1 wt.% NH_4Cl + 1 wt.% NaOH solution at various inhibitor concentrations (line represents EEC fit).

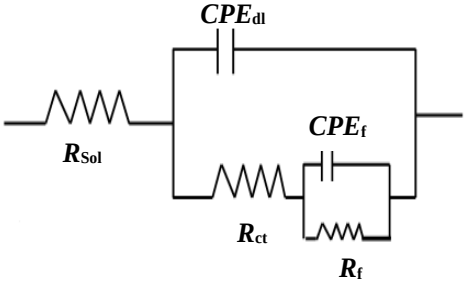

Figure 11. EEC of MS in 1 wt.% NH_4Cl + 1 wt.% NaOH solution at various inhibitor concentrations.

Table 3 shows the EIS fitting parameters. The R_f (film resistance) ascends with ascends in inhibitor concentration and the film is established on the metal surface. R_{ct} value also increases with an increase in inhibitor concentration. Plant extract molecules adsorb onto to MS surface, lowering the C_R. This could be related to the development of a protective coating of inhibitor compounds. The maximum *IE* of ~82% was obtained with 1000 ppm of the extract from the EIS study [29].

The percentage IE_{EIS} of the inhibitor was calculated using the following formula [17]

$$IE(\%) = \frac{R_{ct}^{p} - R_{ct}^{a}}{R_{ct}^{p}} \cdot 100 \tag{10}$$

where, R_{ct}^{a} represent charge transfer resistance without inhibitor and R_{ct}^{p} represent charge transfer resistance with inhibitor.

Table 3. EEC fit parameters for MS with and without inhibitor.

Sr. No.	Conc. (ppm)	R_{sol}, ($\Omega \cdot cm^2$)	Y_1 (cm^{-2})·10^{-5}	n_0	R_f, ($\Omega \cdot cm^2$)	Y_1 (cm^{-2})·10^{-3}	n_1	R_{ct}, ($\Omega \cdot cm^2$)	IE_{EIS}(%)
1	0	52.1	6.7	0.81	194.8	4.2	0.33	906	0
2	200	59.3	5.6	0.84	305	3.6	0.40	1172	22.7
3	400	56.0	5.1	0.83	309.1	4.4	0.36	1305	30.6
4	600	55.8	6.2	0.81	392.9	4.9	0.34	1764	48.6
5	800	55.0	5.7	0.83	395.9	4.6	0.32	1790	49.4
6	1000	60.6	5.1	0.76	482.9	3.9	0.25	5304	82.9

3.4. Adsorption study

Organic compounds tend to resist corrosion because plant extract molecules can adhere to metal surfaces due to their polar properties. Adsorbed water dipoles constantly cover the metal surface in an alkaline solution. The corrodant's accessibility to metal surfaces decreased with the creation of surface layers and films on the metal surface, which was ascribed to the inhibitory effect of organic molecules [30]. Adsorption isotherm has also been used to explain this inhibitory action. Surface coverage (θ) value was determined for various inhibitor concentrations and used for isotherm study. Many isotherms including Langmuir, Temkin, Frumkin and Freundlich models were fitted to this adsorption process. K_{ads} and ΔG_{ads}^{0} values for various isotherms were calculated and are presented in Table 4. Langmuir isotherm is best fitted isotherm with an R^2 value of 0.99 and the plot is shown in Figure 12. The *IE* ascends with the increase in *Azadirachta indica* leaf extract concentration. Thus, the percentage of metal surfaces covered with inhibitor molecules increases due to adsorption [14].

Table 4. K_{ads} and ΔG^0_{ads} values from isotherm study.

Adsorption isotherm	R^2	K_{ads}	ΔG^0_{ads} (kJ/mol)
Temkin	0.9486	0.3316	–14.62
Freundlich	0.9605	0.2144	–13.52
Frumkin	0.9885	0.2084	–13.45

The Langmuir adsorption isotherm equation is shown below (Eq. 11) [30]

$$\frac{C}{\theta} = \frac{1}{K_{ads}} + C \tag{11}$$

where C stands for plant extract concentration in ppm, and K_{ads} represents the adsorption equilibrium constant.

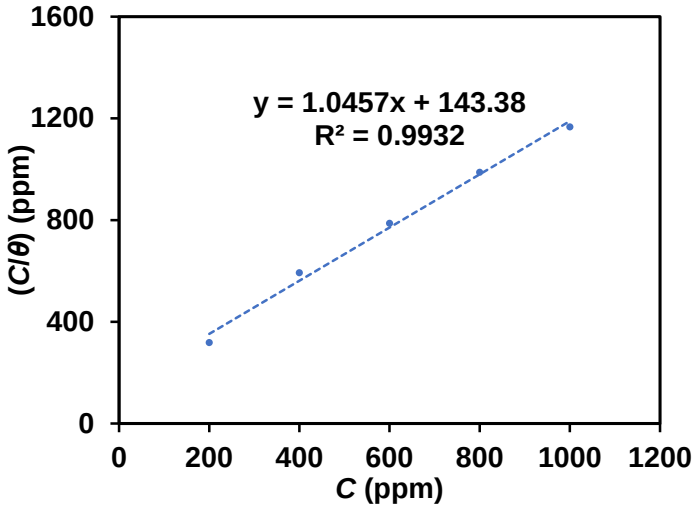

Figure 12. The plot of Langmuir adsorption isotherm for MS in 1 wt.% NH_4Cl + 1 wt.% NaOH with various concentrations of *Azadirachta indica* leaf extract.

The standard free energy of adsorption (ΔG^0_{ads}) associated with adsorption process is given in Eq. 12:

$$\Delta G^0_{ads} = -RT \ln(K_{ads}\rho_W) \tag{12}$$

K_{ads} was found to be 6.97 $L \cdot g^{-1}$ from the Langmuir adsorption isotherm model. Negative ΔG^0_{ads} values show stability and spontaneity of the adsorption mechanism of the adsorbed layer on a metal surface. In this work, the calculated ΔG^0_{ads} for the Langmuir model was –4.893 $kJ \cdot mol^{-1}$, which was less than the threshold (–40 $kJ \cdot mol^{-1}$) for chemisorption. As the value is less than –20 $kJ \cdot mol^{-1}$, the process is physisorption [31].

3.5. Scanning electron microscopy (SEM)

Without plant extract, surface scratches were observed on the MS surface with few pits as seen in Figure 13(a), which corroborates that the metal surface gets corroded with solution. However, *Azadirachta indica* leaf extract improves the surface topography of metal coupons, as seen in Figure 13(b), which confirms the formation of a passive film on the MS surface in 1 wt.% NH_4Cl+ 1 wt.% NaOH solution.

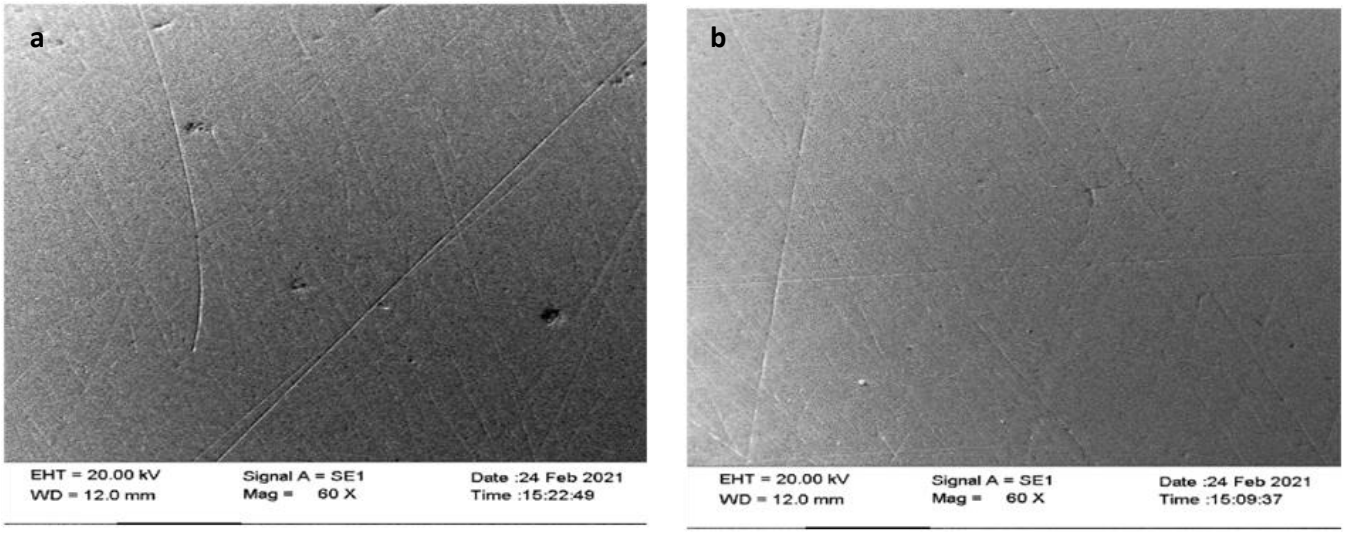

Figure 13. SEM image of MS coupon immersed in alkaline solution (a) without inhibitor (b) with inhibitor.

3.6. FTIR analysis

FTIR analysis of *Azadirachta indica* leaf powder was performed and the obtained spectra are shown in Figure 14. *Azadirachta indica* leaf powder was assorted and grounded with KBr and pressed as a pellet. Bands and peaks provide information about the existing functional groups present in the *Azadirachta indica* leaf powder and were assigned as a strong broad absorbance at 3416.44 cm^{-1} might be O–H and N–H group stretching which is due to the hydroxyl functional group in alcohols, and amides/amines respectively. The absorbance at 1634.86 cm^{-1} indicated the presence of carbonyl functional group stretching in ketones, carboxylic acids and aldehydes. The bands at 1436.04 cm^{-1} and 1050.06 cm^{-1} could be specified as C–O stretching vibrations for fine powder of *Azadirachta indica* leaves [11].

FTIR analysis of the MS coupons immersed in 1 wt.% NH_4Cl + 1 wt.% NaOH solution with and without 1000 ppm inhibitor was performed in the wavenumber range between 4000 and 400 cm^{-1} to classify the functional groups. The study was carried out by immersing an MS metal coupon in 1 wt.% NH_4Cl + 1 wt.% NaOH solution without and with 1000 ppm inhibitor concentration for 6 h. The metal coupon was removed from the test solution, dried with hot air and used for FTIR analysis. Figure 15 illustrates the FTIR spectra of MS coupons withdrawn from a corrosive solution in the absence and presence of *Azadirachta indica* leaf

extract. The FTIR spectra of MS coupon withdrawn from inhibited case showed peaks at 2916.18 cm^{-1}, which denote (C–H stretching vibrations) alkenes, 2367.60 cm^{-1} which signifies to (O–H stretching vibrations) carboxylic acid, 1812.91 cm^{-1}, 1653.85 cm^{-1}, which characterizes (C=O and C=C stretching vibrations) halides and alkane, 1378.55 cm^{-1} and 1013.52 cm^{-1} represents alkenes (C–H bending vibration and C–O vibration) 552 and 685.19 cm^{-1} signifies C=C bending vibration. However, in the case of MS withdrawn from the medium without inhibitor, the spectra show C–H stretching vibration at 2912 cm^{-1} and 2844.79 cm^{-1}, carboxylic acids have been represented by a peak at 2361.48 cm^{-1}, 1538.53 and 1405.06 cm^{-1} indicate the O–H bending vibrations. The extract's spectrum shifts which suggests a reaction between MS and the extract that led to the suppression of corrosion [32].

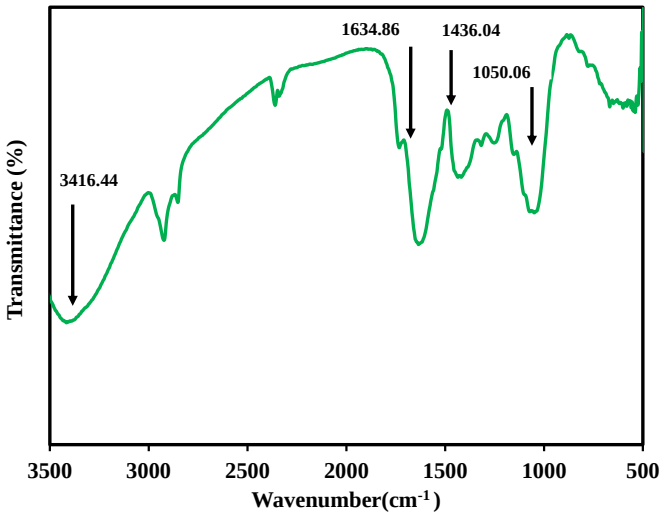

Figure 14. FTIR spectrum of *Azadirachta indica* leaf powder.

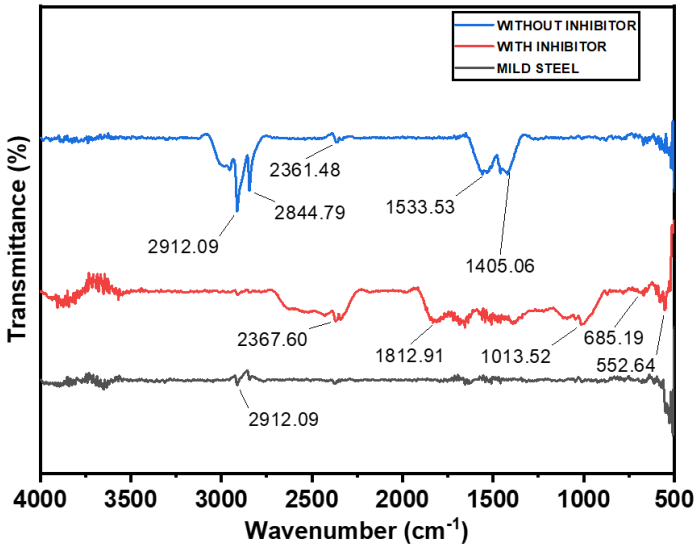

Figure 15. FTIR spectrum of MS coupon, MS immersed in a corrosive medium with and without NLE.

3.7. XPS analysis

Figure 16(a–b) shows the survey scan of XPS spectra of the metal coupons withdrawn from the uninhibited and inhibited case. The survey scan reveals that Fe, O, and C peaks are significant in both cases. Figure 17(a–f) shows the deconvoluted individual spectra of the metal coupons exposed to uninhibited and inhibited mediums. Figures 17a and b show the deconvoluted C1s spectra of MS coupons for both cases. The deconvoluted C1s spectra show two peaks, *viz*., 284.83 and 288.68 eV for both the cases, which corresponds to C=C, O–C=O, and C=N. As seen in Figure 17c and d, two peaks were present in the Fe2p deconvoluted spectra for both cases. The deconvolution of the $Fe2p_{3/2}$ spectrum without the inhibitor case, shows a peak at 710.37 eV, which corresponds to ferric molecules, such as FeOOH and Fe_2O_3 (Fe^{3+} oxide), and for the inhibitor case $Fe2p_{3/2}$ spectrum shows a peak at 710.44 eV. Additionally, a satellite peak is observed for the inhibited case at 712.84 eV in $Fe2p_{3/2}$ spectrum, which is absent in the uninhibited case. $Fe2p_{1/2}$ spectrum shows a peak at 724.02 eV and 724.08 eV for the coupons exposed without and with inhibitor respectively. The finding confirms that the inhibitor molecules adsorb onto the metal surface and provide protection to steel and thus prevent over-oxidation of steel. The inhibitor compounds cause a complex and slow down the corrosion of MS effectively. The XPS spectrum of O1s has two peaks for the coupons exposed to corrosive medium (1 wt.% NH_4Cl + 1 wt.% NaOH) and the plot is shown in Figure 17e and f. Peaks are located at a binding energy of 530.12 eV and 531.8 eV. The O^{2-} the peak of the ferric oxides Fe_2O_3 or/and Fe_3O_4, which indicates the oxygen atom forms coordination with the Fe atoms in both cases. Other peaks at 530.18 and 531.88 eV correspond to OH^- of FeO(OH), which typically appear at 531.7 eV [33].

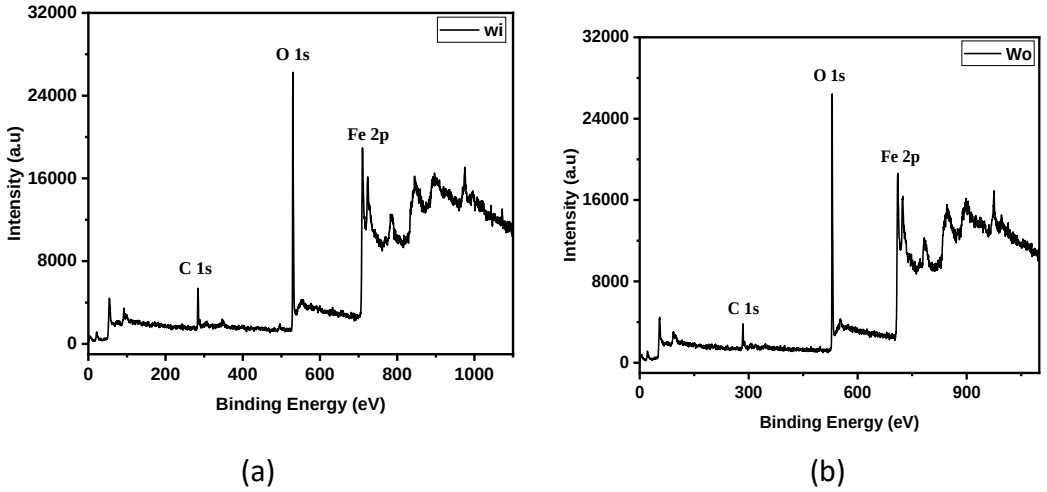

Figure 16. XPS survey scan of MS immersed in 1 wt.% NH_4Cl + 1 wt.% NaOH solution (a) with 1000 ppm *Azadirachta indica* leaf extract concentration (b) without *Azadirachta indica* leaf extract.

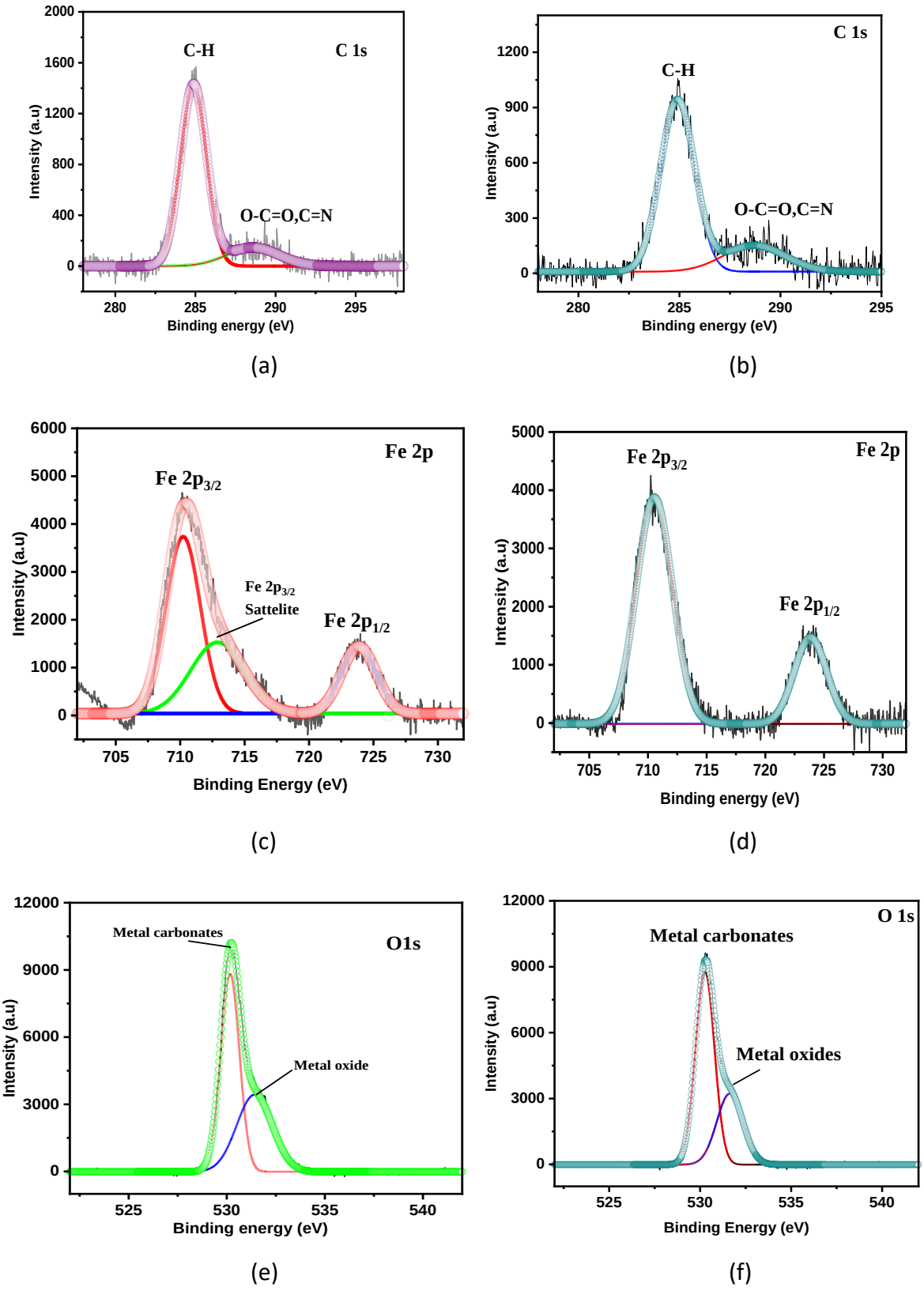

Figure 17. XPS deconvoluted spectra of MS immersed in 1 wt.% NH_4Cl + 1 wt.% NaOH solution with 1000 ppm *Azadirachta indica* leaf extract concentration (a) C1s (c) Fe2p (e) O1s and without *Azadirachta indica* leaf extract concentration (b) C1s (d) Fe2p (f) O1s.

3.8. Chemical reaction and mechanism of corrosion inhibition

In an alkaline solution, a passive film (FeOOH) is formed over MS which decreases the C_R [28].

$$Fe + \frac{1}{2}O_2 + H_2O \rightarrow Fe(OH)_2 \quad (13)$$

$$2Fe(OH)_2 + \frac{1}{2}O_2 \rightarrow 2FeOOH + H_2O \quad (14)$$

However, MS loses its passivation in the presence of Cl^- ions at certain chloride concentrations. Since chloride ions cannot be adsorbed, it breaks down the passive coating, which causes corrosion of MS. Reaction occurs on the MS surface with Cl^- ions. Generally, MS corrodes when it is exposed to Cl^- ions because they generate pitting corrosion, which reduces the resistivity of MS. The reaction taking place on the metal surface is presented (Eq. 13–17).

$$Fe(OH)_2 + 2Cl^- \rightarrow FeOCl_2^{2-} + H_2O \quad (15)$$

$$FeOCl_2^{2-} + H_2O \rightarrow FeCl_2 + 2OH^- \quad (16)$$

From Eq. (16), $FeCl_2$ and OH^- ions are formed at anodic and cathodic sites respectively, which suppresses the dissolution of MS. *Azadirachta indica* leaf contains an amine group ($–NH_2$), which is confirmed by the FTIR analysis. The presence of the amine group in the *Azadirachta indica* leaf is also reported in the literature [34]. With *Azadirachta indica* leaf extract, $FeCl_2$ reacts with the amine group and gets transformed into stable Fe_2O_3, as shown in the reaction (17). The literature claimed that Fe_2O_3 significantly reduces the C_R [35].

$$2FeCl_2 + 4R–NH_2 + 2OH^- + 5O_2 + 2e^- \rightarrow Fe_2O_3 + 4R–Cl + 4NO^- + 5H_2O \quad (17)$$

4. Conclusions

Azadirachta indica leaf inhibitor exhibits excellent corrosion-inhibitory properties in 1 wt.% NH_4Cl + 1 wt.% NaOH solution. Weight loss studies showed that the C_R reduces in the presence of plant extract. *Azadirachta indica* leaf shows outstanding *IE* in alkaline medium containing chloride ions for MS. From the gravimetric study, the highest *IE* of ~82% was obtained with a plant extract concentration of 1000 ppm. A potentiodynamic polarization study revealed that the addition of an *Azadirachta indica* inhibitor to the alkaline medium decreases the corrosion current (i_{corr}) and maximum IE_{Tafel} was obtained as ~85% with 1000 ppm of inhibitor concentration. Electrochemical impedance spectroscopy (EIS) study shows the increase in the resistance with the supplementation of NLE to the corrosive medium. The highest inhibition efficiency of ~83% was obtained from EIS investigations. Among all adsorption isotherm models, the inhibitor best fitted with Langmuir adsorption isotherm. Thermodynamic parameters showed that the inhibitor followed physisorption and

endothermic reaction. SEM images revealed that a relatively better metal surface is obtained in the presence of plant extract and a protecting layer also develops on the MS surface. XPS observation reveals that a phytochemical compound present in the inhibitor forms a complex with an MS surface and thus lowers the corrosion of MS effectively. In the presence of NLE, stable Fe_2O_3 film is formed on the MS surface which causes a decrease in C_R.

References

1. M.E. Mashuga, O.L. Olasunkanmi and E.E. Ebenso, Experimental and theoretical investigation of the inhibitory effect of new pyridazine derivatives for the corrosion of mild steel in 1 M HCl, *J. Mol. Struct*., 2017, **1136**, 127–139. doi: 10.1016/j.molstruc.2017.02.002
2. S.C. Joycee, T. Vidya, S.A. Rattihka, B.S. Prabha, R. Dorothy, T. Sasilatha and S. Rajendran, Corrosion resistance of mild steel in simulated concrete pore solution before and after a paint coating, *Int. J. Corros. Scale Inhib*., 2021, **10**, no. 3, 1323–1335. doi: 10.17675/2305-6894-2021-10-3-28
3. K.K. Anupama and J. Abraham, Electroanalytical studies on the corrosion inhibition behaviour of guava (*Psidium guajava*) leaves extract on mild steel in hydrochloric acid, *Res. Chem. Intermed*., 2013, **39**, 4067–4080. doi: 10.1007/s11164-012-0923-0
4. H.L.Y. Sin, M. Umeda, S. Shironita, A.A. Rahim and B. Saad, *Aquilaria malaccenis* as a green corrosion inhibitor for mild steel in HCl solution, *Int. J. Electrochem. Sci*., 2016, **11**, 7562–7575. doi: 10.20964/2016.09.54
5. M.A. Ameer and A.M. Fekry, Inhibition effect of newly synthesized heterocyclic organic molecules on corrosion of steel in alkaline medium containing chloride, *Int. J. Hydrogen Energy*, 2010, **35**, 11387–11396. doi: 10.1016/j.ijhydene.2010.07.071
6. P.N. Devi, J. Sathiyabama and S. Rajendran, Study of surface morphology and inhibition efficiency of mild steel in simulated concrete pore solution by lactic acid–Zn^{2+} system, *Int. J. Corros. Scale Inhib*., 2017, **6**, no. 1, 18–31. doi: 10.17675/2305-6894-2017-6-1-2
7. B. Xu, W. Yang, Y. Liu, X. Yin, W. Gong and Y. Chen, Experimental and theoretical evaluation of two pyridine carboxaldehyde thiosemicarbazone compounds as corrosion inhibitors for mild steel in hydrochloric acid solution, *Corros. Sci*., 2014, **78**, 260–268. doi: 10.1016/j.corsci.2013.10.007
8. Z.V.P. Murthy and K. Vijayaragavan, Mild steel corrosion inhibition by acid extract of leaves of *Hibiscus sabdariffa* as a green corrosion inhibitor and sorption behaviour, *Green Chem. Lett. Rev*., 2014, **7**, 209–219. doi: 10.1080/17518253.2014.924592
9. R. Subapriya, V. Bhuvaneswari, V. Ramesh and S. Nagini, Ethanolic leaf extract of neem (*Azadirachta indica*) inhibits buccal pouch carcinogenesis in hamsters, *Cell Biochem. Funct*., 2005, **23**, 229–238. doi: 10.1002/cbf.1143
10. K. Biswas, I. Chattopadhyay, R.K. Banerjee and U. Bandyopadhyay, Biological activities and medicinal properties of neem (*Azadirachta indica*), *Curr. Sci*., 2002, **82**, 1336–1345. doi: https://www.jstor.org/stable/24106000

11. S.K. Sharma, A. Mudhoo, G. Jain and E. Khamis, Corrosion inhibition of neem (*Azadirachta indica*) leaves extract as a green corrosion inhibitor for zinc in H_2SO_4, *Green Chem. Lett. Rev*., 2009, **2**, 47–51. doi: 10.1080/17518250903002335
12. T. Dasgupta, S. Banerjee, P.K. Yadava and A.R. Rao, Chemopreventive potential of *Azadirachta indica* (neem) leaf extract in murine carcinogenesis model systems, *J. Ethnopharmacol*., 2004, **92**, 23–26. doi: 10.1016/j.jep.2003.12.004
13. K. Toba, M. Ueyama, K. Kawano and J. Sakai, Corrosion of carbon steel and alloys in concentrated ammonium chloride solutions, *Corrosion*, 2012, **68**, 1049–1056. doi: 10.5006/0587
14. N. Raghavendra and J. Bhat, Chemical components of mature areca nut husk extract as a potential corrosion inhibitor for mild steel and copper in both acid and alkali media, *Chem. Eng. Commun*., 2018, **205**, 145–160. doi: 10.1080/00986445.2017.1370709
15. P. Ramakrishnan, V. Janardhanan, R. Sreekumar and K. Mohan, Investigation on the effect of green inhibitors for corrosion protection of mild steel in 1 M NaOH solution, *Int. J. Corros*., 2014, 487103, 1–5. doi: 10.1155/2014/487103
16. M. Adebayo, S. Akande, A. Olorunfemi, O. Ajayi, J. Orege and E. Daniel, Equilibrium and thermodynamic characteristics of the corrosion inhibition of mild steel using sweet prayer leaf extract in alkaline medium, *Prog. Chem. Biochem*., 2021, **4**, 80–91. doi: 10.22034/pcbr.2021.120449
17. O. Akinbulumo, O. Odejobi and E. Odekanle, Thermodynamics and adsorption study of the corrosion inhibition of mild steel by *Euphorbia heterophylla L*. extract in 1.5 M HCl, *Results Mater*., 2020, **5**, 100074. doi: 10.1016/j.rinma.2020.100074
18. R.D. Salim, Q.A. Jawad, K.S. Ridah, L.M. Shaker, A.A. Al-Amiery, A.A.H. Kadhum and M.S. Takriff, Corrosion inhibition of thiadiazole derivative for mild steel in hydrochloric acid solution, *Int. J. Corros. Scale Inhib*., 2020, **9**, no. 2, 550–561. doi: 10.17675/2305-6894-2020-9-2-10
19. A.J.M. Eltmimi, A. Alamiery, A.J. Allami, R.M. Yusop, A.H. Kadhum and T. Allami, Inhibitive effects of a novel efficient Schiff base on mild steel in hydrochloric acid environment, *Int. J. Corros. Scale Inhib*., 2021, **10**, no. 2, 634–648. doi: 10.17675/2305-6894-2021-10-2-10
20. Yu.I. Kuznetsov, N.N. Andreev and S.S. Vesely, Why do we reject papers with calculations of inhibitor adsorption based on data on protective effects?, *Int. J. Corros. Scale Inhib*., 2015, **4**, no. 1, 108–109. doi: 10.17675/2305-6894-2015-4-1-108-109
21. V.I. Vigdorovich, L.E. Tsygankova, E.D. Tanygina, A.Y. Tanygin and N.V. Shel, Preservative materials based on vegetable oils for steel protection against atmospheric corrosion I. Colza oil, *Int. J. Corros. Scale Inhib*., 2016, **5**, no. 1, 59–65. doi: 10.17675/2305-6894-2016-5-1-5

22. M.T. Majd, G. Bahlakeh, A. Dehghani, B. Ramezanzadeh and M. Ramezanzadeh, Combined molecular simulation, DFT computation and electrochemical studies of the mild steel corrosion protection against NaCl solution using aqueous eucalyptus leaves extract molecules linked with zinc ions, *J. Mol. Liq*., 2019, **294**, 111550. doi: 10.1016/j.molliq.2019.111550
23. M. Dahmani, E. Abdelkader, S. Al-Deyab, B. Hammouti and A. Bouyanzer, Corrosion inhibition of C38 steel in 1 M HCl: A comparative study of black pepper extract and its isolated piperine, *Int. J. Electrochem. Sci*., 2010, **5**, 1060–1069. doi: 10.1016/S1452-3981(23)15344-2
24. R. Solmaz, G. Kardas, B. Yazıc and M. Erbil, Adsorption and corrosion inhibitive properties of 2-amino-5-mercapto-1,3,4-thiadiazole on mild steel in hydrochloric acid media, *Colloids Surf., A*, 2008, **312**, 7–17. doi: 10.1016/j.colsurfa.2007.06.035
25. S.N. Victoria, R. Prasad and R. Manivannan, *Psidium guajava* leaf extract as green corrosion inhibitor for mild steel in phosphoric acid, *Int. J. Electrochem. Sci*., 2015, **10**, 2220–2238. doi: 10.1016/S1452-3981(23)04842-3
26. M.A. Ameer, A.M. Fekry, A.A. Ghoneim and F.A. Attaby, Electrochemical corrosion inhibition of steel in alkaline chloride solution, *Int. J. Electrochem. Sci*., 2010, **5**, 1847–1861. doi: 10.1016/S1452-3981(23)15389-2
27. L.Y.S. Helen, A.A. Rahim, B. Saad, M.I. Saleh and P.B. Raja, *Aquilaria crassna* leaves extracts – A green corrosion inhibitor for mild steel in 1 M HCl medium, *Int. J. Electrochem. Sci*., 2014, **9**, 830–846. doi: 10.1016/S1452-3981(23)07760-X
28. A. Sadkowski, Unusual electrochemical immittance spectra with negative resistance and their validation by Kramers–Kronig transformation, *Solid State Ionics*, 2005, **176**, 1987–1996. doi: 10.1016/j.ssi.2004.08.041
29. H. Xu, K. Shen, S. Liu, L. Zhang, X. Wang, J. Qin and W. Wang, High activity methanol/H_2O_2 catalyst of nanoporous gold from Al–Au ribbon precursors with various circumferential speeds, *J. Phys. Chem*., 2016, **120**, 25296–25305. doi: 10.1021/acs.jpcc.6b06314
30. A. Hamdy and N. El-Gendy, Thermodynamic, adsorption and electrochemical studies for corrosion inhibition of carbon steel by henna extract in acid medium, *Egypt. J. Pet*., 2013, **22**, 17–25. doi: 10.1016/j.ejpe.2012.06.002
31. S.O. Adejo, M.M. Ekwenchib, J.A. Gbertyoa, T. Menengea and J.O. Ogbodo, Determination of adsorption isotherm model best fit for methanol leaf extract of *Securinega virosa* as corrosion inhibitor for corrosion of mild steel in HCl, *J. Adv. Chem*., 2014, **10**, 2737–2742. doi: 10.24297/jac.v10i5.891
32. D. Li, P. Zhang, X. Guo, X. Zhao and Y. Xu, The inhibition of mild steel corrosion in 0.5 M H_2SO_4 solution by radish leaf extract, *RSC Adv*., 2019, **9**, 40997–41009. doi: 10.1039/C9RA04218K

33. Y. Tang, F. Zhang, H. Shengxiang, C. Ziyi, W. Zhenglei and J. Wenheng, Novel benzimidazole derivatives as corrosion inhibitors of mild steel in the acidic media. Part I: Gravimetric, electrochemical, SEM and XPS studies, *Corros. Sci*., 2013, **74**, 271–282. doi: 10.1016/j.corsci.2013.04.053
34. H.S. Ryu, J.K. Singh, H.S. Lee, M.A. Ismail and W.J. Park, Effect of $LiNO_2$ inhibitor on corrosion characteristics of steel rebar in saturated $Ca(OH)_2$ solution containing NaCl: An electrochemical study, *Constr. Build. Mater*., 2017, **133**, 387–396. doi: 10.1016/j.conbuildmat.2016.12.086
35. J.K. Singh and D.D.N. Singh, The nature of rusts and corrosion characteristics of low alloy and plain carbon steels in three kinds of concrete pore solution with salinity and different pH, *Corros. Sci*., 2012, **56**, 129–142. doi: 10.1016/j.corsci.2011.11.012

♦ ♦ ♦